Available online at www.sciencedirect.com
SCIENCE DIRECT
Biochemical and Biophysical Research Communications 344 (2006) 315–322
BBRC
www.elsevier.com/locate/ybbrc

Crystal structures of the catalytic domain of human stromelysin-1 (MMP-3) and collagenase-3 (MMP-13) with a hydroxamic acid inhibitor SM-25453 ☆

Tetsuya Kohno [a,*], Hitoshi Hochigai [a], Eiki Yamashita [b], Tomitake Tsukihara [b], Masaharu Kanaoka [a]

[a] *Drug Research Division, Dainippon Sumitomo Pharma Co., Ltd., 3-1-98 Kasugadenaka, Konohana-ku, Osaka 554-0022, Japan*
[b] *Institute for Protein Research, Osaka University, 3-2 Yamada-oka, Suita, Osaka 565-0871, Japan*

Received 12 March 2006
Available online 27 March 2006

Abstract

Crystal structures of the catalytic domain of human stromelysin-1 (MMP-3) and collagenase-3 (MMP-13) with a hydroxamic acid inhibitor SM-25453 have been solved at 2.01 and 2.37 Å resolutions, respectively. The results revealed that the binding modes for this inhibitor to MMP-3 and -13 were quite similar. However, subtle comparative differences were observed at the bottom of S1′ pockets, which were occupied with the guanidinomethyl moiety of the inhibitor. A remarkable feature of the inhibitor was the deep penetration of its long aliphatic chain into the S1′ pocket and exposure of the guanidinomethyl moiety to the solvent.

Keywords: MMP-3; Stromelysin-1; MMP-13; Collagenase-3; X-ray crystallography; Hydroxamic acid inhibitor

Matrix metalloproteases (MMPs), a class of zinc-containing enzymes, play crucial roles in physiological and pathological degradation of mammalian extracellular matrix in a variety of tissues including breast tumors and osteoarthritis cartilage. To date, more than 20 MMPs have been identified [1] and classified according to their substrate specificities; namely, collagenases, stromelysins, gelatinases, and membrane-bound MT-MMPs. MMPs are expressed as inactive proenzymes with three distinct structural domains: N-terminal propeptide, which contains approximately 80 residues, is cleaved for enzyme activation; zinc-containing central domain, which contains approximately 170–180 residues, holds full catalytic activity; and C-terminal hemopexin-like domain, which contains approximately 190 residues, is inferred to be responsible for the recognition of extracellular matrix and alignment of the catalytic domain at the enzymatic cleavage site [2].

Collagenase-3 (MMP-13: EC 3.4.24.B4) preferentially cleaves collagen type I, II, and III, fibronectin, and aggrecan which are major components of cartilage. Stromelysin-1 (MMP-3: EC 3.4.24.17) plays the role as an initiator to activate other MMP proenzymes, including MMP-13, by cleaving the propeptides. Both MMP-3 and -13 are overexpressed in rheumatoid arthritis (RA) and osteoarthritis (OA) cartilages, whereas MMP-13 gene expression is not detected in normal human tissues [3]. Therefore, these enzymes are considered as potential therapeutic targets for RA and OA, and some drug candidates are under clinical test [4,5].

There have been a number of reports on the structure of the catalytic domain of human MMP-3 solved by NMR and X-ray crystallography, with a variety of inhibitors [6–26]. On the other hand, only a few are reported on human MMP-13 with inhibitors solved by NMR [27,28] and X-ray [29], perhaps because of its thermal instability

☆ *Abbreviations:* MMP, matrix metalloprotease; PDB, Protein Data Bank; RMSD, root-mean-square deviation.

* Corresponding author. Fax: +81 6 6466 5459.
E-mail address: tetsuya-kono@ds-pharma.co.jp (T. Kohno).

0006-291X/$ - see front matter © 2006 Elsevier Inc. All rights reserved.
doi:10.1016/j.bbrc.2006.03.098

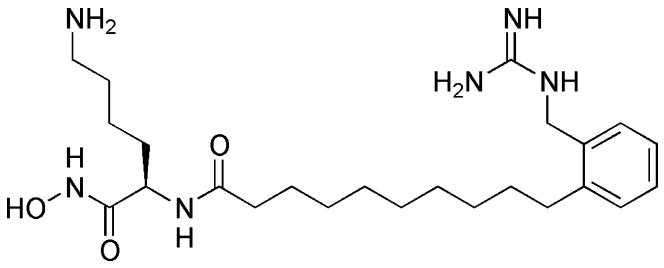

Fig. 1. Chemical structure of SM-25453.

and autolysis-prone nature. Although all MMP structures reported to date have similar 3D folds, there are distinct substrate specificities between these enzymes. Understanding the differences, especially in substrate binding sites, is important to design selective inhibitors.

SM-25453 (Fig. 1) was identified as a potent MMP-3 and -13 inhibitor in the course of screening a therapeutic drug for OA with a selectivity between MMPs ($K_i = 5.6$ μM for MMP-1, 0.02 μM for MMP-3, and 0.007 μM for MMP-13). The structure of SM-25453 consists of a hydroxamic acid, D-lysine, and a long aliphatic chain with a hydrophilic guanidinomethyl moiety at the end, which presumably binds to the hydrophobic S1′ pocket. To understand how these structural features contribute to the potency and specificity of SM-25453, we set out to analyze the structures of the inhibitor–enzyme complexes. Here, we report X-ray crystal structures of the catalytic domains of both MMP-3 and -13 with SM-25453 at 2.01 and 2.37 Å resolutions, respectively.

Materials and methods

Protein expression and purification. C-terminal truncated form of proMMP-3 was overexpressed in *Escherichia coli* BL21/DE3 cells, purified and activated to the mature form (residues Phe83-Pro256) by the published procedures [30,31]. C-terminal truncated form of proMMP-13 (residues Leu20-Gly267) was overexpressed in *E. coli* BL21/DE3 transformed with the pET3a-proMMP-13 vector by the published procedures of mouse MMP-13 catalytic domain [32]. The inclusion body of the overexpressed protein was solubilized in buffer A (6 M guanidine HCl, 50 mM Tris–HCl, pH 7.5) and refolded by dialysis against buffer B (150 mM NaCl, 5 mM $CaCl_2$, 0.5 mM $ZnCl_2$, and 20 mM Tris–HCl, pH 8.0) at 4 °C. The protein was purified by a HiLoad 26/10 SP Sepharose column (Amersham Biosciences). The purified proMMP-13 was concentrated with Centriprep YM-10 (Millipore) and activated by treatment with 1 mM 4-aminophenylmercuric acetate (APMA) for 2 h at 37 °C, to produce the mature form (residues Tyr104-Asn274). The mature MMP-13 was purified by a HiPrep 16/60 Sephacryl S-100 HR column (Amersham Biosciences).

Crystallization. A 2:1 molar ratio of the inhibitor SM-25453 over the purified protein was added immediately after purification to prevent further degradation. The mixture was concentrated to 20–25 mg/ml using Centriprep YM-10 (Millipore) and crystallized using hanging drop vapor diffusion method. For MMP-3, diffraction quality crystals were grown against the reservoir consisting of 40% PEG4000, 5% MPD, and 0.1 M Hepes, pH 7.5, at 20 °C. The crystals grew to maximum dimensions of approximately 0.8 mm in diameter in 10 days. For MMP-13, diffraction quality crystals were grown against the reservoir consisting of 0.8 M potassium sodium tartrate tetrahydrate, 0.1 M Hepes, pH 7.5, at 4 °C. The crystals grew to maximum dimensions of approximately $0.8 \times 0.5 \times 0.5$ mm in 5 days.

Data collection, processing, phasing, and crystallographic refinement. X-ray diffraction data of MMP-3 and -13 complexed with SM-25453 were collected on the DIP-2020 (Mac Science) and Rigaku R-AXIS IV, respectively. The diffraction images were processed with MOSFLM and scaled using SCALA in the CCP4 program suite [33]. The structures of MMP-3 and -13 complexed with SM-25453 were solved by the molecular replacement with AMORE [34] using the 83–255 residues of proMMP-3 (PDB code: 2SRT [6]), and the MMP-13 complexed with RS-113456 (PDB code: 830C [29]) as the search models, respectively. Crystallographic refinement was carried out with CNS [35] using the combination of maximum likelihood and simulated annealing by torsion angle molecular dynamics [36]. Free R values (R_{free}) were used for cross validation [37]. The $2F_o - F_c$ and $F_o - F_c$ electron density maps showed good density for the inhibitor structures in the S1′ pockets. After several rounds of refinement, water molecules were added to the models. The model building was performed using the program O [38]. The inhibitor model was built using Quanta (Accerlys) and geometry was parameterized using XPLO-2D [39]. The stereochemistry of the models was verified using PROCHECK [40]. The results of X-ray diffraction data collection and refinement statistics are presented in Table 1.

The atomic coordinates of MMP-3 and MMP-13 with SM-25453 have been deposited in PDB as accession numbers 2D1O and 2D1N, respectively.

Results and discussion

Structure of MMP-3/SM-25453 complex

The crystal structure of MMP-3 complexed with SM-25453 was determined and refined as summarized in Table 1. Quality of the MMP-3 crystals was high as they diffracted at 1.7 Å resolution or higher without using synchrotron radiation. The present model has two zinc ions and three calcium ions in each crystallographically independent subunit. The geometry of the current model was such that the root-mean-square deviations (RMSDs) from ideal values are 0.006 Å for bond lengths and 1.2° for bond angles. According to the Ramachandran plot [41], 89.5% of non-glycine and non-proline residues have their ψ and ϕ angles in the most favored region, and 9.1% are in the additional allowed region, whereas Arg149 and Asn162 are in disallowed regions, even though their electron density was very clear. There are two molecules (molecules A and B) in an asymmetric unit. The C-terminal residues, from Asp251 to Pro253, are well defined in electron density in molecule A, but disordered in molecule B, because the C-terminus of molecule A is bound to a part of active-site cleft of other crystallographic symmetry related molecules, whereas that of molecule B does not contact with any other and is exposed to the solvent.

The overall structure of the catalytic domain of MMP-3 was essentially identical with that previously reported, consisting of three α-helices (α1, Lys110 to Glu125; α2, Leu195 to Leu208; α3, Asp256 to Tyr246), four parallel β-sheet strands (β1, Thr95 to Val102; β2, Thr131 to Leu135; β3, Ile142 to Ala147; and β5, Ala178 to Asp182), and one anti-parallel β-strand (β4, Leu164 to Ala167), which were identified by PROCHECK analysis. However, the conformation of the flexible loop which forms the outer part of the S1′ pocket, differed significantly from other reported

Table 1
Data collection and crystallographic refinement statistics

	MMP-3/SM-25453	MMP-13/SM-25453
Data collection statistics		
X-ray source	Rotating anode generator RU-300 (Rigaku)	Rotating anode generator ultraX18 (Rigaku)
Detector instrument	DIP-2020 (Mac Science)	*R*-axis IV (Rigaku)
Wavelength (Å)	1.5418	1.5418
Resolution range (outer shell) (Å)	10–2.01 (2.12–2.01)	10–2.37 (2.52–2.37)
Space group	*C*2	$P3_2$
Cell dimensions (Å, °)	$a = 105.36$, $b = 50.95$, $c = 80.79$, $\alpha = 90°$, $\beta = 105.00°$, $\gamma = 90°$	$a = 99.47$, $b = 99.47$, $c = 67.52$, $\alpha = 90°$, $\beta = 90°$, $\gamma = 120°$
Molecules in asymmetric unit	2	2
Total observed reflections	92414	88,944
Unique reflections used	26846	27,744
R_{merge} (%)	5.1(8.8)	8.1(78.8)
Completeness (%)	96.7(79.2)	97.3(93.0)
Refinement statistics		
R_{cryst} (%)	18.3(19.4)	21.8(37.5)
R_{free} (%)	20.6(22.4)	23.9(37.5)
No. of water molecules	205	49
RMSD		
Bond length (Å)	0.005	0.008
Bond angles (°)	1.1	1.2

$R_{merge} = \Sigma_{hkl}|\langle I\rangle - I|/\Sigma_{hkl}|I|$.
$R_{cryst} = \Sigma_{hkl}||F_{obs}| - |F_{calc}||/\Sigma_{hkl}|F_{obs}|$, where F_{obs} and F_{calc} are the observed and calculated structure factor amplitudes, respectively.
$R_{free} = \Sigma_{hkl}||F_{obs}| - |F_{calc}||/\Sigma_{hkl}|F_{obs}|$, calculated from 5% of all the data that were not used in the refinement.

structures. The hydroxamic acid binds within the active site by coordinating with the catalytic zinc atom with two hydroxamate oxygen atoms and three imidazole nitrogen atoms from His201, His205, and His211(Figs. 2A and 3A). The hydroxamate nitrogen seems to be protonated and have an interaction with the carbonyl oxygen of Ala165. The carbonyl oxygen of SM-25453 is positioned to form hydrogen bond interaction with the amide nitrogen of Leu164. These interactions are same as those of the hydroxamic acid inhibitors reported previously.

A remarkable feature of SM-25453 is the deep penetration of the long aliphatic chain into the S1′ pocket and exposure of the guanidinomethyl moiety to the solvent.

Compared with other reported structures with inhibitors having long P1′ side chain (1hfs [10], 1b8y, 1caq, 1c1z [18], 1c8t, 1c3 [23], and 1g4k [24]), there is a significant difference in the conformation of His224 to Leu228. This difference was induced by the stacking interaction between the guanidinomethyl moiety and the side chain of His224 from the asymmetric related molecule. The two parts are parallel to

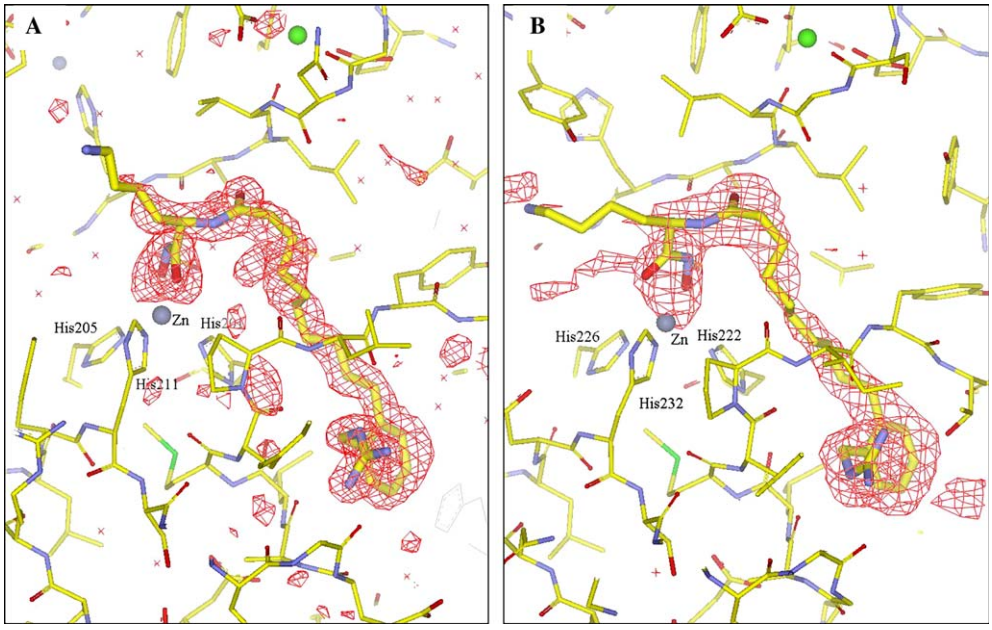

Fig. 2. The $F_o - F_c$ omit electron density map around SM-25453 bound in (A) MMP-3, (B) MMP-13 active sites. Both densities are contoured at 3.0σ.

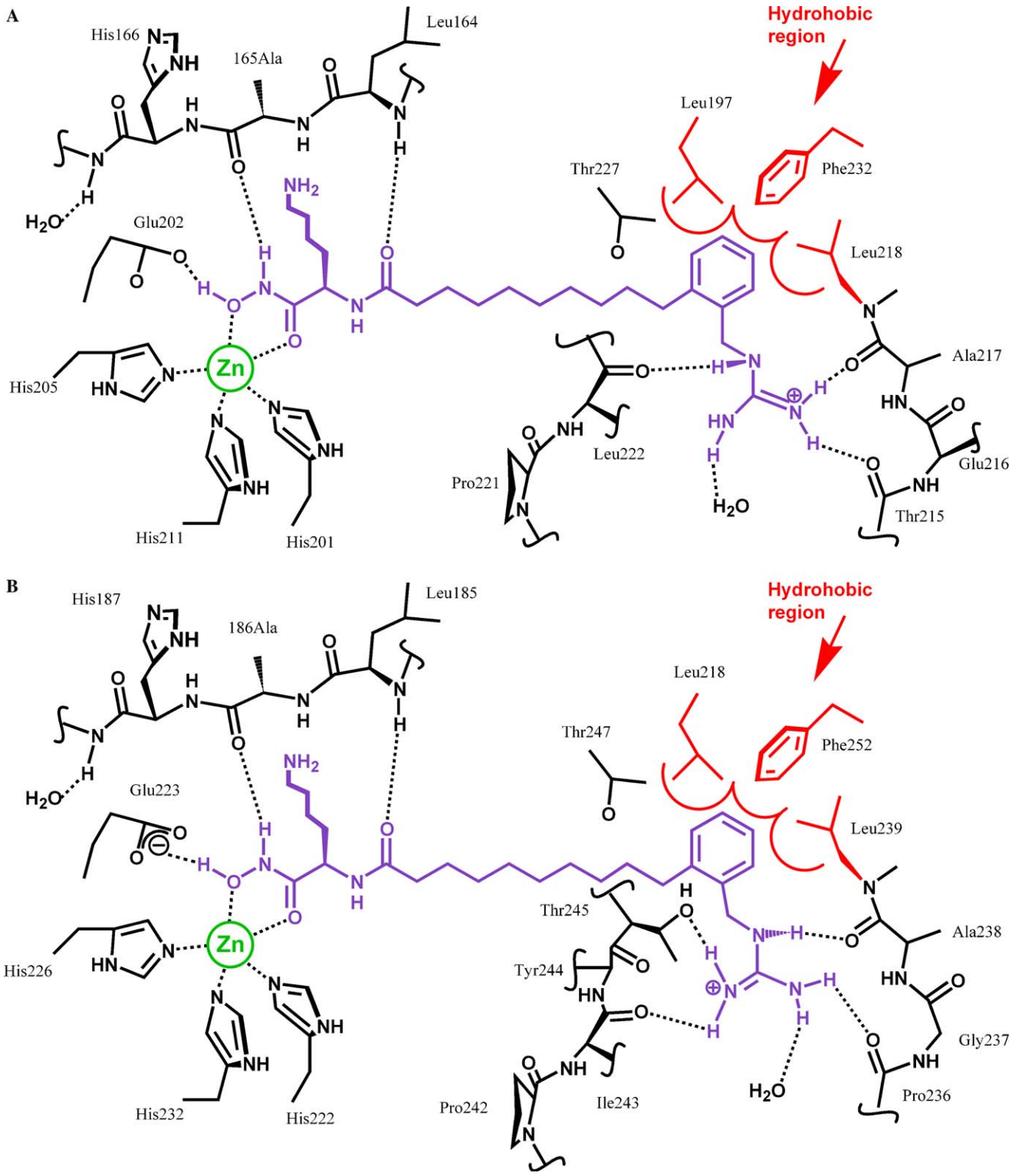

Fig. 3. Schematic drawings of interactions between SM-25453 and (A) MMP-3, and (B) MMP-13. Main hydrogen bonds are indicated by broken lines and hydrophobic contacts are represented as red lines (amino acid residues are also in red). (For interpretation of the references to colour in this figure legend, the reader is referred to the web version of this paper.)

each other. This interaction seems to be an important factor to form the asymmetric dimer.

The phenyl ring of SM-25453 is positioned at the bottom of S1′ pocket, interacts with Leu218 and Phe232 on one side, and with Leu197 and Thr227, members of the flexible loops, on the outside of the S1′ pocket (Fig. 3A).

The S1′ pocket contains several carbonyl oxygen atoms that could serve as hydrogen bond acceptors, but only

structures with hydrophobic P1′ side chain have been reported so far. The hydrophilic guanidinomethyl of SM-25453, however, has three hydrogen bond interactions; Nε of guanidinomethyl interacts with the carbonyl oxygen of Leu222 of the S1′ flexible loop, each Nη atom interacts with carbonyl oxygen atom of Thr215 or Ala217. Consequently, the other Nη atom interacts with a solvent molecule (Fig. 3A).

Structure of MMP-13/SM-25453 complex

The crystal structure of MMP-13 complexed with SM-25453 was also determined and refined as summarized in Table 1. The present model has three zinc ions and three calcium ions in each crystallographically independent subunit. Two of the zinc ions were positioned similar to those in MMP-3 (a catalytic and a structural zincs), and the third was found between molecules A and B, interacting with Glu135, His157, and two water molecules. This third zinc ion seems to play the role of a connector between molecules A and B. The geometry of the current model is such that the RMSDs from ideal values are 0.008 Å for bond lengths and 1.2° for bond angles. The Ramachandran plot indicates that 88.3% of non-glycine and non-proline residues are in the most favored region, and 10.2% are in the additional allowed region, whereas Lys170 and Asn 194 are in disallowed regions. The sequence alignment (Fig. 4) and superimposing of the structures of MMP-3 and -13 (Fig. 5) show that Lys170 of MMP-13 and Arg149 of MMP-3, which are both in disallowed region, are located in similar positions and both are determined unambiguously with clear electron density. In addition, Asn 194 and Gly 183 of MMP-13 and Gly173 and Asn162 of MMP-3 are also in similar positions, respectively. Therefore, these disallowed conformations were not due to insufficient refinement, but should be a common structural feature of MMP-3 and -13.

The core domain of MMP-13 consists of three α-helices (α1, His131 to Ser146; α2, Leu216 to Leu228; and α3, Asp256 to Tyr266), four parallel β-sheet strands (β1, Met116 to Val123; β2, Asn152 to Leu156; β3, Ile163 to Gly168; and β5, Ala199 to Asp202), and one anti-parallel β-strand (β4, Leu185 to Ala188). The S1′ flexible loop including Gly248 to His251, which were not defined in previously reported X-ray data[29], showed well-defined electron density, unveiling the detailed difference in ligand binding sites between MMP-3 and -13.

```
stromelysin-1  83   FRTFPGIPKW RKTHLTYRIV NYTPDLPKDA VDSAVEKALK VWEEVTPLTF
collagenase-3  104  YNVFPRTLKW SKMNLTYRIV NYTPDMTHSE VEKAFKKAFK VWSDVTPLNF
                    .  **   **  * .****** *****.    *. *  **.* ** .**** *

stromelysin-1  133  SRLYEGEADI MISFAVREHG DFYPFDGPGN VLAHAYAPGP GINGDAHFDD
collagenase-3  154  TRLHDGIADI MISFGIKEHG DFYPFDGPSG LLAHAFPPGP NYGGDAHFDD
                    .** .* *** ****...*** ********.  .****..***    *******

stromelysin-1  183  DEQWTKDTTG TNLFLVAAHE IGHSLGLFHS ANTEALMYPL YHSLTDLTR-
collagenase-3  204  DETWTSSSKG YNLFLVAAHE FGHSLGLDHS KDPGALMFPI YT--YTGKSH
                    ** **  . *  ********* .****** **   .  ***.*. *

stromelysin-1  232  FRLSQDDING IQSLYGPPPD SP
collagenase-3  252  FMLPDDDVQG IQSLYGPG-
                      *..**. * *******
```

Fig. 4. Sequence alignment of the catalytic domains of human stromelysin-1 (MMP-3) and collagenase-3 (MMP-13). α-Helices are indicated in red, β-sheets are shown in blue. "*" indicates identical residues and "." indicates similar residues. (For interpretation of the references to colour in this figure legend, the reader is referred to the web version of this paper.)

The binding mode of SM-25453 to MMP-13 is quite similar to that to MMP-3. The hydroxamic acid moiety coordinates with the catalytic zinc atom with two oxygen atoms and three imidazole nitrogen atoms from His226, His222, and His232 (Figs. 2B and 3B). The hydroxamate nitrogen of the inhibitor seems to be protonated and have an interaction with the carbonyl oxygen of Ala186. The carbonyl oxygen of SM-25453 is positioned to form hydrogen bond interaction with amide nitrogen of Leu185. The phenyl ring moiety has interactions with the hydrophobic region at the bottom of S1′ pocket composed of Leu218, Leu239, and Phe252. One of Nη atoms of the guanidinomethyl moiety seems to be protonated and have interactions with Oγ atom of Thr245 and the carbonyl oxygen of Ile243 in S1′ flexible loop. The other Nη atom has interactions with the carbonyl oxygen of Pro236 and with a solvent molecule. Nε of the guanidinomethyl moiety has an interaction with the carbonyl oxygen of Ala238 (Fig. 3B).

Comparison with other reported MMP-13 structures (1fls [28], 456c, 830c [29]) by superimposing backbone atoms showed remarkable conformational similarity except for N-terminal residues (Tyr104 to Arg109), even though the structure of the bound ligand is different, especially the guanidinomethyl moiety. Probably because the S1′ flexible loop of MMP-13 is one residue shorter than MMP-3 (Fig. 4), the conformational change in MMP-13 by ligand binding is not as large as that in MMP-3.

Comparison of the MMP-3 and MMP-13 structures complexed with SM-25453

The structures of MMP-3 and -13, including the bound conformations of SM-25453, are largely similar (Figs. 2 and 5A), so that the backbone atoms can be superimposed with 0.64 Å RMSD. However, there are some differences, particularly in the S1′ flexible loop, as evident by sequence alignment (Fig. 4) and structural superposition (Fig. 5B).

The X-ray structures determined in this study revealed that the binding conformations of the hydroxamic acid moiety with both MMP-3 and -13 were quite similar, whereas those of D-lysine side chain were not as similar. This part protrudes out of the active-site cleft into the solvent and does not make notable interactions with the proteins. As a consequence it should be flexible since the electron density maps were unclear (Fig. 2).

The long aliphatic chain plays the role as a linker which connects the hydroxamic acid moiety and the guanidinomethyl moiety. The length of this part is important for the selectivity of MMPs [42], by distinguishing between the types with a large and open pocket

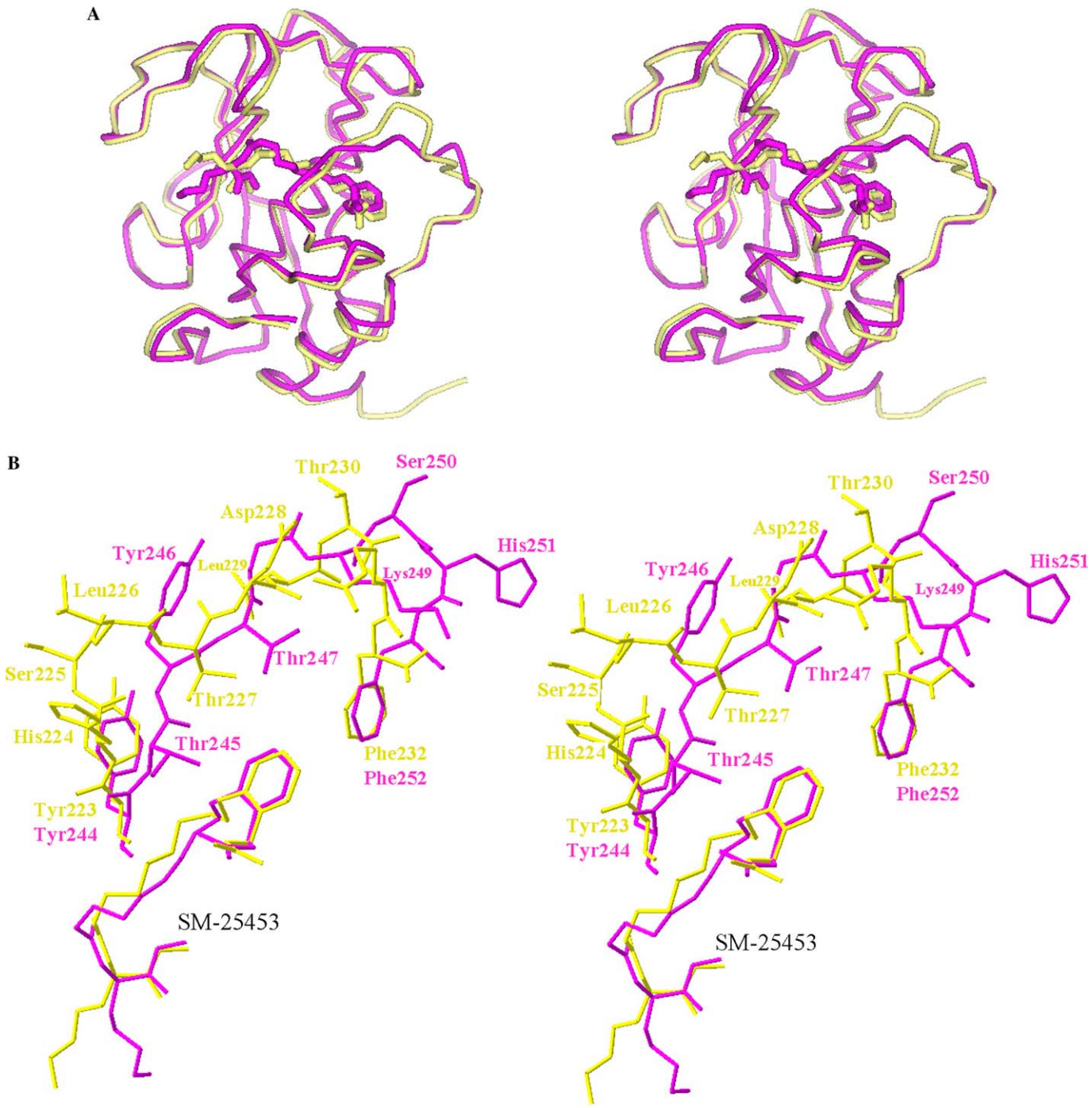

Fig. 5. Stereo view of superposition of MMP-3 (yellow) and -13 (pink) with SM-25453 bound in the active sites (A) Cα trace models, (B) S1′ flexible loops (Tyr223 to Phe232 of MMP-3 and Tyr244 to Phe252 of MMP-13) and bound SM-25453. (For interpretation of the references to colour in this figure legend, the reader is referred to the web version of this paper.)

(MMP-3, -8, and -13), and those with a small and closed pocket (MMP-1 and -7).

Structural superposition analysis revealed that the phenyl ring moieties of Phe232 of MMP-3 and Phe252 of MMP-13, both are members of S1′ flexible loop, were similarly positioned (Fig. 5B), even though the conformations of the S1′ flexible loops including these residues differ greatly, influenced by amino acid differences and crystallographic packing interaction. It seems that binding interaction of the phenyl moiety of SM-25453 and the phenyl rings of these residues are important for structural stabilization of both MMP-3 and -13. In contrast, the binding interactions of guanidinomethyl moiety are different between MMP-3 and -13. In MMP-13, we observed four hydrogen bond interactions: one of the Nη atoms has interactions with two residues of the S1′ flexible loop (Oγ atom of Thr245 and carbonyl oxygen of Ile243) and the other Nη atom has an interaction with the carbonyl oxygen of Pro236.

Nε of the guanidinomethyl moiety has an interaction with the carbonyl oxygen of Ala238 (Fig. 3B). On the other hand, in MMP-3, we observed three hydrogen bond interactions: only one of Nη atoms has interactions with the carbonyl oxygen atoms of Thr215 and Ala217, which are structurally equivalent to Pro236 and Ala238 of MMP-13, respectively (Fig. 3A). The other Nη atom has an interaction with the carbonyl oxygen of Leu222 in counter direction to that of MMP-13 (Fig. 3A). The binding affinity of SM-25453 with MMP-13 is approximately three times higher than that with MMP-3. These structural differences might have resulted in the affinity difference.

The X-ray structures determined in this study revealed the details of the inhibitor-enzyme interactions at the bottom of S1′ pockets of both MMP-3 and MMP-13. The binding interactions of the guanidinomethyl moiety of SM-25453 are quite unique and provide the difference in inhibitor–enzyme interactions between MMP-3 and MMP-13.

Further research and development of SM-25453 itself as a therapeutic for OA has been discontinued, but the structure information obtained through this study, particularly the hydrophilic nature of S1′ pocket, is useful for designing follow-up compounds.

Conclusions

The crystal structures of both recombinant human MMP-3 and MMP-13 complexed with a hydroxamic acid inhibitor SM-25343 were determined. Comparison of the structures revealed that the protein structures and the bound conformations of hydroxamic group of the inhibitor were largely similar, but the S1′ flexible loops and the conformations of guanidinomethyl moiety of the inhibitor were different.

Acknowledgments

We thank G. Hashimoto for construction of recombinant MMP-13 plasmid, F. Samizo for synthesis of SM-25453.

References

[1] M.D. Sternlicht, Z. Werb, How matrix metalloproteinases regulate cell behavior, Annu. Rev. Cell Dev. Biol. 17 (2001) 463–516.
[2] U. Gohlke, F.X. Gomis-Ruth, T. Crabbe, G. Murphy, A.J. Docherty, W. Bode, The C-terminal (heamopexin-like) domain structure of human gelatinase A (MMP2): structural implications for its function, FEBS Lett. 378 (1996) 126–130.
[3] D. Wernicke, C. Seyfert, B. Hinzmann, E. Gromnica-Ihle, Cloning of collagenase 3 from the synovial membrane and its expression in rheumatoid arthritis and osteoarthritis, J. Rheumatol. 23 (4) (1996) 590–595.
[4] D.R. Close, Matrix metalloproteinase inhibitors in rheumatic diseases, Ann. Rheum. Dis. 60 (Suppl 3) (2001) 62–67.
[5] J.B. Catterall, T.E. Cawston, Drugs in development: bisphosphonates and metalloproteinase inhibitors, Arthritis Res. Ther. 5 (2003) 12–24.
[6] P.R. Gooley, J.F. O'Connell, A.I. Marcy, G.C. Cuca, S.P. Salowe, B.L. Bush, J.D. Hermes, C.K. Esser, W.K. Hagmann, J.P. Springer, B.A. Johnson, The NMR structure of the inhibited catalytic domain of human stromelysin-1, Nat. Struct. Biol. 1 (1994) 111–118.
[7] S.R. Van Doren, A.V. Kurochkin, W. Hu, Q.Z. Ye, L.L. Johnson, D.J. Hupe, E.R. Zuiderweg, Solution structure of the catalytic domain of human stromelysin complexed with a hydrophobic inhibitor, Protein Sci. 4 (1995) 2487–2498.
[8] J.W. Becker, A.I. Marcy, L.L. Rokosz, M.G. Axel, J.J. Burbaum, P.M. Fitzgerald, P.M. Cameron, C.K. Esser, H.W.K. Agmann, J.D. Hermes, J.P. Springer, Stromelysin-1: three-dimensional structure of the inhibited catalytic domain and of the C-truncated proenzyme, Protein Sci. 4 (1995) 1966–1976.
[9] F.X. Gomis-Ruth, K. Maskos, M. Betz, A. Bergner, R. Huber, K. Suzuki, N. Yoshida, H. Nagase, K. Brew, G.P. Bourenkov, H. Bartunik, W. Bode, Mechanism of inhibition of the human matrix metalloproteinase stromelysin-1 by TIMP-1, Nature 389 (1997) 77–81.
[10] C.K. Esser, R.L. Bugianesi, C.G. Caldwell, K.T. Chapman, P.L. Durette, N.N. Girotra, I.E. Kopka, T.J. Lanza, D.A. Levorse, M. MacCoss, K.A. Owens, M.M. Ponpipom, J.P. Simeone, R.K. Harrison, L. Niedzwiecki, J.W. Becker, A.I. Marcy, M.G. Axel, A.J. Christen, J. McDonnell, V.L. Moore, J.M. Olszewski, C. Saphos, D.M. Visco, F. Shen, A. Colletti, P.A. Krieter, W.K. Hagmann, Inhibition of stromelysin-1 (MMP-3) by P1′-biphenylylethyl carboxyalkyl dipeptides, J. Med. Chem. 40 (1997) 1026–1040.
[11] B.J. Stockman, D.J. Waldon, J.A. Gates, T.A. Scahill, D.A. Kloosterman, S.A. Mizsak, E.J. Jacobsen, K.L. Belonga, M.A. Mitchell, B. Mao, J.D. Petke, L. Goodman, E.A. Powers, S.R. Ledbetter, P.S. Kaytes, G. Vogeli, V.P. Marshall, G.L. Petzold, R.A. Poorman, Solution structures of stromelysin complexed to thiadiazole inhibitors, Protein Sci. 7 (1998) 2281–2286.
[12] B.C. Finzel, E.T. Baldwin, G.L. Bryant Jr., G.F. Hess, J.W. Wilks, C.M. Trepod, J.E. Mott, V.P. Marshall, G.L. Petzold, R.A. Poorman, T.J. O'Sullivan, H.J. Schostarez, M.A. Mitchell, Structural characterizations of nonpeptidic thiadiazole inhibitors of matrix metalloproteinases reveal the basis for stromelysin selectivity, Protein Sci. 7 (1998) 2118–2126.
[13] S. Pikul, K.L. Mcdow Dunham, N.G. Almstead, B. De, M.G. Natchus, M.V. Anastasio, S.J. Mcphail, C.E. Snider, Y.O. Taiwo, T. Rydel, C.M. Dunaway, F. Gu, G.E. Mieling, Discovery of potent, achiral matrix metalloproteinase inhibitors, J. Med. Chem. 41 (1998) 3568–3571.
[14] Y.C. Li, X. Zhang, R. Melton, V. Ganu, N.C. Gonnella, Solution structure of the catalytic domain of human stromelysin-1 complexed to a potent, nonpeptidic inhibitor, Biochemistry 37 (1998) 14048–14056.
[15] M.G. Natchus, M. Cheng, C.T. Wahl, S. Pikul, N.G. Almstead, R.S. Bradley, Y.O. Taiwo, G.E. Mieling, C.M. Dunaway, C.E. Snider, J.M. McIver, B.L. Barnett, S.J. McPhail, M.B. Anastasio, B. De, Design and synthesis of conformationally constrained MMP inhibitors, Bioorg. Med. Chem. Lett. 8 (1998) 2077–2780.
[16] M.Y. Cheng, M.G. Natchus, B. De, N.G. Almstead, S. Pikul Design, Synthesis and biological evaluation of matrix metalloproteinase inhibitors derived from a modified proline scaffold, J. Med. Chem. 42 (1999) 5426–5436.
[17] N.G. Almstead, R.S. Bradley, S. Pikul, B. De, M.G. Natchus, Y.O. Taiwo, F. Gu, L.E. Williams, B.A. Hynd, M.J. Janusz, C.M. Dunaway, G.E. Mieling, Design, synthesis, and biological evaluation of potent thiazine-and thiazepine-based matrix metalloproteinase inhibitors, J. Med. Chem. 42 (1999) 4547–4562.
[18] A.G. Pavlovsky, M.G. Williams, Q.Z. Ye, D.F. Ortwine, C.F. Purchase 2nd, A.D. White, V. Dhanaraj, B.D. Roth, L.L. Johnson, D.J. Hupe, C. Humblet, T.L. Blundell, X-Ray structure of human stromelysin catalytic domain complexed with nonpeptide inhibitors: implications for inhibitor selectivity, Protein Sci. 8 (1999) 1455–1462.
[19] L. Chen, T.J. Rydel, C.M. Dunaway, S. Pikul, K.M. Dunham, F. Gu, B.L. Barnett, Crystal structure of the stromelysin catalytic domain at

2.0Å resolution: inhibitor-induced conformational changes, J. Mol. Biol. 293 (1999) 545–557.
[20] M.Y. Cheng, B. De, S. Pikul, N.G. Almstead, M.G. Natchus, M.V. Anastasio, S.J. Mcphail, C.E. Snider, Y.O. Taiwo, L.Y. Chen, M. Dunaway, F. Gu, M.E. Dowty, G.E. Mieling, M.J. Janusz, S. Wang-Weigand, Design and synthesis of piperazine-based matrix mettalloproteinase inhibitors, J. Med. Chem. 43 (2000) 369–380.
[21] M.G. Natchus, R.G. Bookland, B. De, N.G. Almstead, S. Pikul, Development of new hydroxamate matrix metalloproteinase inhibitors derived from functionalized 4-aminoprolines, J. Med. Chem. 43 (2000) 4948–4963.
[22] M.G. Natchus, R.G. Bookland, M.J. Laufersweiler, S. Pikul, N.G. Almstead, B. De, M.J. Janusz, L.C. Hsieh, F. Gu, M.E. Pokross, V.S. Patel, S.M. Garver, S.X. Peng, T.M. Branch, S.L. King, T.R. Baker, D.J. Foltz, G.E. Mieling, Development of new carboxylic acid-based Mmp inhibitors derived from functionalized propargylglycines, J. Med. Chem. 44 (2001) 1060–1071.
[23] D.L. Steele, O. El-Kabbani, P. Dunten, L.J. Windsor, R.U. Kammlott, R.L. Crowther, C. Michoud, J.A. Engler, J.J. Birktoft, Expression, characterization and structure determination of an active site mutant (Glu202-Gln) of mini-stromelysin-1, Protein Eng. 13 (2000) 397–405.
[24] P. Dunten, U. Kammlott, R. Crowther, W. Levin, L.H. Foley, P. Wang, R. Palermo, X-Ray structure of a novel matrix metalloproteinase inhibitor complexed to stromelysin, Protein Sci. 10 (2001) 923–926.
[25] S. Pikul, K.M. Dunham, N.G. Almstead, B. De, M.G. Natchus, Y.O. Taiwo, L.E. Williams, B.A. Hynd, L.C. Hsieh, M.J. Janusz, F. Gu, G.E. Mieling, Heterocycle-based MMP inhibitors with P2′ substituents, Bioorg. Med. Chem. Lett. 11 (2001) 1009–1013.
[26] S. Arumugam, S.R. Van Doren, Global orientation of bound MMP-3 and N-TIMP-1 in solution via residual dipolar couplings, Biochemistry 42 (2003) 7950–7958.
[27] X. Zhang, N.C. Gonnella, J. Koehn, N. Pathak, V. Ganu, R. Melton, D. Parker, S.I. Hu, K.Y. Nam, Solution structure of the catalytic domain of human collagenase-3 (MMP-13) complexed to a potent non-peptidic sulfonamide inhibitor: binding comparison with stromelysin-1 and collagenase-1, J. Mol. Biol. 301 (2000) 513–524.
[28] F.J. Moy, P.K. Chanda, J.M. Chen, S. Cosmi, W. Edris, J.I. Levin, R. Powers, High-resolution solution structure of the catalytic fragment of human collagenase-3 (MMP-13) complexed with a hydroxamic acid inhibitor, J. Mol. Biol. 302 (2000) 671–689.
[29] B. Lovejoy, A.R. Welch, S. Carr, C. Luong, C. Broka, R.T. Hendricks, J.A. Campbell, K.A. Walker, R. Martin, H. Van Wart, M.F. Browner, Crystal structures of MMP-1 and -13 reveal the structural basis for selectivity of collagenase inhibitors, Nat. Struct. Biol. 6 (1999) 217–221.
[30] A.I. Marcy, L.L. Eiberger, R. Harrison, H.K. Chan, N.I. Hutchinson, W.K. Hagmann, P.M. Cameron, D.A. Boulton, J.D. Hermes, Human fibroblast stromelysin catalytic domain: expression, purification, and characterization of a C-terminally truncated form, Biochemistry 30 (1991) 6476–6483.
[31] P.R. Gooley, B.A. Johnson, A.I. Marcy, G.C. Cuca, S.P. Salowe, W.K. Hagmann, C.K. Esser, J.P. Springer, Secondary structure and zinc ligation of human recombinant short-form stromelysin by multidimensional heteronuclear NMR, Biochemistry 32 (1993) 13098–13108.
[32] V. Lemaître, A. Jungbluth, Y. Eeckhout, The recombinant catalytic domain of mouse collagenase-3 depolymerizes type I collagen by cleaving its aminotelopeptides, Biochem. Biophys. Res. Commun. 230 (1997) 202–205.
[33] Collaborative Computational Project, Number 4. The CCP4 suite: programs for protein crystallography, Acta Cryst. D 50 (1994) 760–763.
[34] J. Navaza, Implementation of molecular replacement in AMoRe, Acta Cryst. D57 (2001) 1367–1372.
[35] A.T. Brünger, P.D. Adams, G.M. Clore, W.L. DeLano, P. Gros, R.W. Grosse-Kunstleve, J.S. Jiang, J. Kuszewski, M. Nilges, N.S. Pannu, R.J. Read, L.M. Rice, T. Simonson, G.L. Warren, Crystallography & NMR system: a new software suite for macromolecular structure determination, Acta Cryst. D54 (1998) 905–921.
[36] P.D. Adams, N.S. Pannu, R.J. Read, A.T. Brünger, Cross-validated maximum likelihood enhances crystallographic simulated annealing refinement, Proc. Natl. Acad. Sci. USA 94 (1997) 5018–5023.
[37] A.T. Brünger, Free *R* value: a novel statistical quantity for assessing the accuracy of crystal structures, Nature 355 (1992) 472–475.
[38] T.A. Jones, J.Y. Zou, S.W. Cowan, M. Kjeldgaard, Improved methods for building protein models in electron density maps and the location of errors in these models, Acta Cryst. A47 (1991) 110–119.
[39] G.J. Kleywegt, T.A. Jones, Model building and refinement practice, Methods Enzymol. 277 (1997) 208–230.
[40] R.A. Laskowski, M.W. MacArthur, D.S. Moss, J.M. Thornton, PROCHECK: a program to check the stereochemical quality of protein structures, J. Appl. Cryst. 26 (1993) 283–291.
[41] G.N. Ramachandran, C. Ramakrishnan, V. Sasisekharan, Stereochemistry of polypeptide chain configurations, J. Mol. Biol. 7 (1963) 95–99.
[42] A.R. Welch, C.M. Holman, M. Huber, M.C. Brenner, M.F. Browner, H.E.V. Wart, Understanding the P1′ specificity of the matrix metalloproteinases: effect of S1′ pocket mutations in matrilysin and stromelysin-1, Biochemistry 35 (1996) 10103–10109.